Nat Hazards (2016) 84:821–849
DOI 10.1007/s11069-016-2453-3

ORIGINAL PAPER

A multi-dimensional statistical rainfall threshold for deep landslides based on groundwater recharge and support vector machines

A. Vallet[1,2] · D. Varron[3] · C. Bertrand[2] · O. Fabbri[2] · J. Mudry[2]

Received: 7 February 2015 / Accepted: 4 July 2016 / Published online: 12 July 2016

Abstract The rainfall threshold determination is widely used for estimating the minimum critical rainfall amount which may trigger slope failure. The aim of this study was to develop an objective approach for the determination of a statistical rainfall threshold of a deep-seated landslide. The determination is based on recharge estimation and a multi-dimensional rainfall threshold. This new method is compared with precipitation and with a conventional 'two-dimensional' rainfall threshold. The method is designed to be semiautomatic, enabling an eventual integration into a landslide warning system. The method consists in two independent parts: (i) unstable event identification based on displacement time series and (ii) multi-dimensional rainfall threshold determination based on support vector machines. The method produces very good results and constitutes an appropriate tool to define an objective and optimal rainfall threshold. In addition to shortened computation times, the non-necessity of pre-requisite hypotheses and a fully automatic implementation, the newly introduced multi-dimensional approach shows performances similar to the classical two-dimensional approach. This shows its relevance and its

✉ A. Vallet
a.vallet@brgm.fr

D. Varron
davit.varron@univ-fcomte.fr

C. Bertrand
catherine.bertrand@univ-fcomte.fr

O. Fabbri
olivier.fabbri@univ-fcomte.fr

J. Mudry
jacques.mudry@univ-fcomte.fr

[1] Parc scientifique et industriel, BRGM, 21 A rue Alain Savary, 25000 Besançon Cedex, France

[2] UMR6249 Chrono-Environnement, Université Bourgogne - Franche-Comté, 16 route de Gray, 25030 Besançon Cedex, France

[3] UMR6623 Laboratoire de Mathématiques de Besançon, Université Bourgogne - Franche-Comté, 16 route de Gray, 25030 Besançon Cedex, France

suitability to define a rainfall threshold. Lastly, this study shows that the recharge is a relevant parameter to be taken into account for deep-seated rainfall-induced landslides. Using the recharge rather than the precipitation significantly improves the delineation of a rainfall threshold separating stable and unstable events. The performance and accuracy of the multi-dimensional rainfall threshold developed for the Séchilienne landslide make it an appropriate method for integration into the present-day landslide warning system.

Keywords Rainfall threshold · Support vector machines · Groundwater recharge · Deep-seated landslide · Probability · Early warning system

1 Introduction

The determination of a rainfall threshold is a widely used method for estimating the minimum critical rainfall amount which may result in slope failure (Wilson and Wieczorek 1995; Terlien 1998; Vita et al. 1998; Wieczorek and Guzzetti 1999; Iverson 2000; Aleotti 2004; Guzzetti et al. 2008; Frattini et al. 2009). This tool, first established by Caine (1980), is mainly used for shallow landslides. Rainfall thresholds can be defined either by empirical (statistical) or by deterministic (physical based) approaches, at local or at regional scales. The rainfall threshold identifies the boundary which separates rainfall conditions which do or do not cause slope destabilization. Although landslide warning systems can be based on various data (landslide displacement velocity, micro-seismic activity monitoring, rockfall, etc.), only rainfall thresholds allow predictions to be made, due to the availability of weather forecasts. This association reinforces the prominent role that rainfall thresholds play in slope failure alert system.

Elevated pore water pressure, induced by the recharge of groundwater hydrosystems, is one of the main triggering factors of deep-seated landslides (Iverson 2000; Rutqvist and Stephansson 2003; Bogaard et al. 2007; Bonzanigo et al. 2007). However, the relationship between groundwater level and destabilization rate is complex for deep-seated landslides (Rutqvist and Stephansson 2003; Binet et al. 2007; Berti et al. 2012). In addition, for deep-seated landslides involving groundwater flow, the groundwater recharge, rather than precipitation, is a relevant parameter to consider (Vallet et al. 2015a). Lastly, the identification of stable and unstable events, on which the rainfall threshold definition is based, is difficult for continuously moving landslides. To the best of our knowledge, no attempts to define an empirical rainfall threshold to a deep-seated landslide (>100 m) have been successfully undertaken (Zhang et al. 2006).

Most studies dealing with rainfall thresholds are biased since thresholds are usually determined visually or with poor mathematical or statistical bases (Terlien 1998; Guzzetti et al. 2007; Segoni et al. 2014). In addition, the identification of the stable or unstable events along with the determination of the associated rainfall conditions mainly rely on subjective decisions (Terlien 1998; Segoni et al. 2014). An objective definition of the threshold, which minimizes false-positive or false-negative occurrences, is fundamental to integrate rainfall thresholds as a warning system tool.

The aim of this study is to develop an objective approach for the determination of a statistical rainfall threshold for deep-seated landslides. The determination is based on the estimation of recharge and on the definition of a multi-dimensional rainfall threshold. This new approach will be compared with precipitation and with a classical 'two-dimensional' rainfall threshold. It is designed to be semiautomatic, enabling an eventual integration into a landslide warning system. It is based on a daily time step and consists in two independent

parts which can be used together or separately, according to the user's requirements and according to the site constraints. These two parts are: (1) a semiautomatic identification of stable/unstable events based on displacement velocity time series and (2) a determination of a multi-dimensional rainfall threshold based on support vector machines (SVM), a linear classifier related to the statistical learning theory (Fig. 1). Preliminary results of this research have been presented at the IAEG XII Congress (Vallet et al. 2015d).

2 Strategy for the definition of an optimal and objective rainfall threshold suitable for deep-seated landslides

The rainfall threshold quantifies the minimal rainfall conditions supposed to trigger slope destabilization. The definition of the rainfall threshold is based on a historical inventory either of only unstable events (the so-called one-class label threshold) or of both stable and

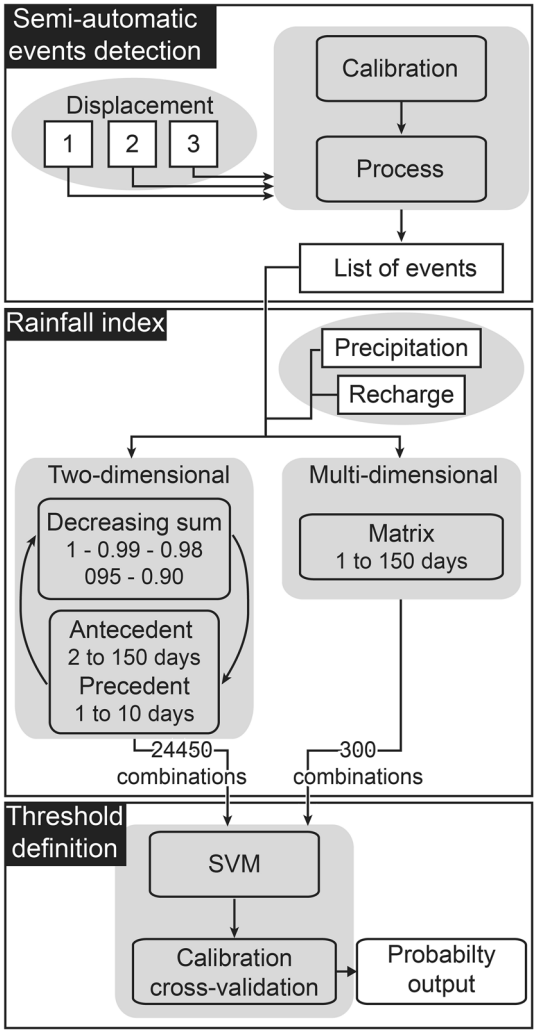

Fig. 1 Workflow of the method to determine the rainfall threshold for the two-dimensional (Sect. 4.1) and the multi-dimensional (Sect. 4.2) approaches, based on precipitation or recharge estimates. The rainfall threshold is defined using the support vector machines (SVM) method (Appendix) of which the list of events is determined by a semiautomatic event detection method (Sect. 3)

unstable events (the so-called two-class label threshold). For any event, the rainfall conditions, also referred to as the rainfall index, are classically on the basis of two parameters. As such, the classical index is referred to as a two-dimensional index. The literature presents various combinations of indexes (Guzzetti et al. 2007, 2008), among which the most used are rainfall intensity and duration, or daily rainfall and antecedent rainfall. The selection of the rainfall index depends mainly on the landslide settings (landslide type, climate conditions, geomorphology, etc.).

2.1 Rainfall threshold in the case of deep-seated landslides

The complex structural geology and the complex groundwater hydrodynamics of deep-seated landslides generally involve complicated hydro-mechanical relationships between precipitation and deformation (Terlien 1998; Cappa et al. 2004; Binet et al. 2007; Berti et al. 2012). For deep-seated landslides, threshold deterministic approaches based on hydro-mechanical models are difficult to implement or to calibrate because of the scarcity or absence of measured hydrodynamic parameters such as groundwater levels or spring flows in the disturbed areas (Guzzetti et al. 2007). Therefore, in the case of large amounts of available data, the definition of a statistical local threshold (specific to a landslide) is preferred since it can implicitly take into account these relationships (Guzzetti et al. 2007). The statistical threshold method is an efficient method by which the rainfall threshold can be simply and unambiguously determined from the data and does not require extensive investigations. In addition, there is no need for an *a priori* knowledge of the hydro-mechanical behavior of the landslide to propose valid predictions. Using a statistical approach rather than a deterministic approach provides a truly objective method for the stakeholders managing the warning system.

Geomorphological, geological and hydrogeological characteristics play key roles in the destabilization of deep-seated landslides (Peruccacci et al. 2012). In addition, although the deep-seated landslide destabilization is mainly controlled by a rainfall trigger (short-term component), site-specific time-dependent factors (long-term components) such as creep deformation or slope groundwater hydraulic connectivity modifications can also be significant (Rutqvist and Stephansson 2003; Corominas et al. 2005; Berti et al. 2012). For these reasons, global thresholds are not suitable for landslides which are strongly influenced by site characteristics other than the rainfall trigger. In these cases, a local threshold which implicitly takes into account the landslide characteristics is more adequate (Guzzetti et al. 2008)

The inertia and the buffering hydraulic properties of the groundwater reservoir triggering the deep-seated landslide destabilization can significantly smooth short-term fluctuations such as the intensity or the duration of rainfall events (Terlien 1998; Van Asch et al. 1999; Nafarzadegan et al. 2012). The landslide aquifer hydrodynamical response is therefore more influenced by the antecedent rainfall (which takes into account multiple rainfall events over a long period) than it would be by a single rainfall event (Martelloni et al. 2012). Therefore, the commonly used daily rainfall–antecedent rainfall index is more suitable for deep-seated landslide studies. The daily rainfall amount can be replaced by a period not necessarily limited to one day, hereafter named precedent rainfall amount (Fig. 2a). This choice is justified by the fact that a single rainfall day will not have a significant influence on destabilization for a large deep-seated landslide (Van Asch et al. 1999). Lastly, Vallet et al. (2015a) showed that the recharge is a more suitable parameter than the precipitation to be considered for deep-seated landslides. The recharge is therefore a relevant parameter to take into account to establish a rainfall threshold.

2.2 Rainfall conditions: from two-dimensional to multi-dimensional rainfall index

Classically, rainfall thresholds are determined with a two-dimensional rainfall index. For deep-seated landslides, the definition of the two-dimensional rainfall index requires the choices of the cumulative method (decreasing or conventional sum, decay method and decay factor) and of the period extent (Terlien 1998). These choices are subjective and may depend on the actual knowledge of the landslide–rainfall relationship, with the possibility of missing the best combination (among the numerous possible combinations), that is the combination which maximizes the discrimination between stable and unstable events. The proposed multi-dimensional method is based on a multi-dimensional rainfall index (MDI). The MDI is built for each identified event, whatever stable or unstable. The index dimension is the number of days of the investigated period preceding a given event. The rainfall amount of each day will be a value of the MDI (Fig. 2b). For example, for a given event and a given period of 15 days (preceding the event), the dimension of the MDI will be 15 and the rainfall amount of each day will be one value of the MDI which can be seen as a point in a 15-dimension space with rainfall amount as coordinate values. This approach allows an objective determination of the rainfall conditions associated with an event. It, however, requires a mathematical tool able to classify multi-dimensional datasets.

2.3 Mathematical classifier tool for an optimal definition of the rainfall threshold

Recent studies (Guzzetti et al. 2007; Brunetti et al. 2010; Berti et al. 2012; Peruccacci et al. 2012) determined an optimal rainfall threshold using Bayesian statistical approaches or frequentist methods which, in addition to threshold identification, allow an estimation of landslide failure probabilities. The probability estimates are a great advantage for threshold

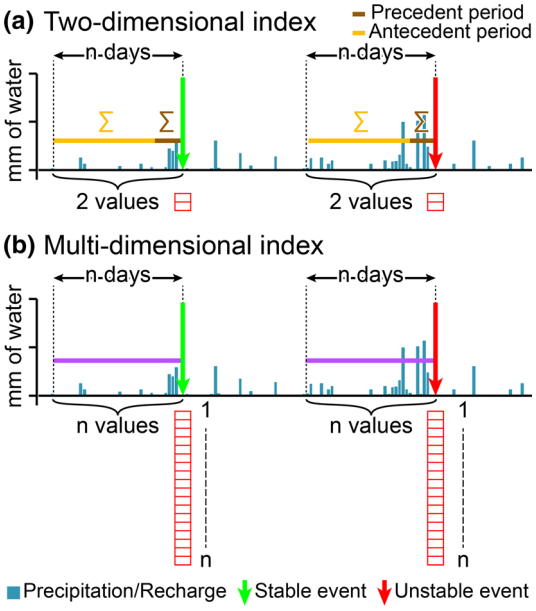

Fig. 2 Method of determination of the rainfall indexes in the case (**a**) of two-dimensional approach and (**b**) of multi-dimensional approach

definition where data quality and rainfall–displacement complex relationships can lead to significant uncertainties (Berti et al. 2012). Moreover, precipitation is not the only factor that causes destabilization or failure (Aleotti and Chowdhury 1999). A probabilistic approach allows to take into account the uncertainties in the rainfall–destabilization relationship.

The Bayesian approach was tested in recent studies (Guzzetti et al. 2007; Brunetti et al. 2010; Berti et al. 2012). However, the support vector machines method (SVM classifier), a supervised learning method, is chosen here to determine the optimal rainfall threshold. The SVM classifier is characterized by a higher accuracy than other classifying methods (Ben-Yacoub 1999; Huang et al. 2003). Furthermore, the SVM classifier is a widely available tool on various software platforms (Ivanciuc 2007) and is easy to implement and to calibrate (Cristianini 2000; Hsu et al. 2003; Ben-Hur and Weston 2010). For studies where landslide probability assessment is important, even though it is a non-probabilistic binary linear classifier, SVM add-ins (complementary functionalities) are developed for producing probabilistic estimates dependent on the SVM classifier (Platt 1999; Lin et al. 2007). Most rainfall threshold mathematical studies (Brunetti et al. 2010; Peruccacci et al. 2012; Martelloni et al. 2012) are based only on unstable events (one-class rainfall threshold) and do not take into account stable events. Although the SVM classifier was initially designed to classify two-class datasets, a new SVM formulation for a one-class classification problem was developed (Schölkopf et al. 1999; Tax and Duin 2004) and is suitable for such studies. Lastly, for the new threshold approach using a multi-dimensional rainfall index, the SVM classifier demonstrated a better performance for classification (Huang et al. 2003; Byvatov et al. 2003). For all these reasons, the SVM classifier is considered here as the best solution, being generic and being easily implemented as an objective tool by stakeholders in landslide warning systems.

2.4 Stable or unstable event detection

The use of a mathematical tool to define a rainfall threshold is not sufficient to warrant an operational applicability for an early warning system. Indeed, the identification of the stable/unstable events needs also to be based on an objective and reproducible method. For continuously moving landslides without any historical acceleration crisis catalog, it is relevant to use a velocity criterion method based on displacement velocity time series in order to detect acceleration crises (peaks) and periods of rests (troughs) accounting for unstable and stable events, respectively.

Peak/trough identification is a classical task in signal processing and in time series analysis. A commonly used identification method is based on the derivative of the data series and looks for downward-going zero crossings. However, in a natural dataset, a random noise can cause false zero crossings, leading to incorrect peak/trough detections. To avoid this bias, data series are often smoothed to remove random noise, resulting in signal information loss (O'Haver 1997; Palshikar 2009). Generally, the more generic the method, the more necessary it is to inform input parameters. Generic methods can be too general to fit to specific signal properties (non-periodic signal, trend, amplitude, etc.) or to detect only given peak/trough patterns. On the contrary, methods which require few input parameters (Excoffier and Guiochon 1982; Li et al. 1995; Jacobson 2001) are usually restricted to a specific domain of application.

Generally, deep-seated landslide displacement velocities present random peak/trough location distributions and random peak/trough properties with a large range of widths, amplitudes and shapes. Most of the peaks/troughs of the displacement velocity time series

are asymmetrical. In addition, displacement velocity signals can be considered to be relatively noisy, considering that not all peaks/troughs match with an unstable landslide event and have to be filtered according to the definition of the events. None of the above-mentioned methods are suitable to account for the displacement velocity signal characteristics and for the detection requirements. In this contribution, a method is specifically designed with the aim to be applicable to any other deep-seated landslide sites.

3 The semiautomatic event detection method

Most deep-seated landslides are continuously moving, and it is not possible to identify stable or unstable events. Therefore, the choice is made here to define a critical statistical threshold defining the minimal amount of rainfall (precipitation or recharge) which results in a significant increase in slope destabilization. Based on the displacement velocity time series, two types of events are defined: low-destabilization (LD) events and high-destabilization (HD) events.

3.1 Definition of LD and HD events

In this study, LD and HD events are defined following a simple statistical indicator (quartile) and a data series pattern (peak or trough) based on the displacement velocity time series. The LD events must be inferior to the first quartile and must match a trough. The HD events must be superior to the third quartile and must match a peak. Because displacement velocities are measured locally, an event is considered as representative of landslide destabilization only if it is identified on a selected set of displacement measurement devices. In the cases where several stations are required, an event is considered as representative only if it is identified on all selected stations within a 10-day margin (spatial and temporal coincidence). The event date is then defined as the barycentre of the various event dates identified on each displacement velocity time series.

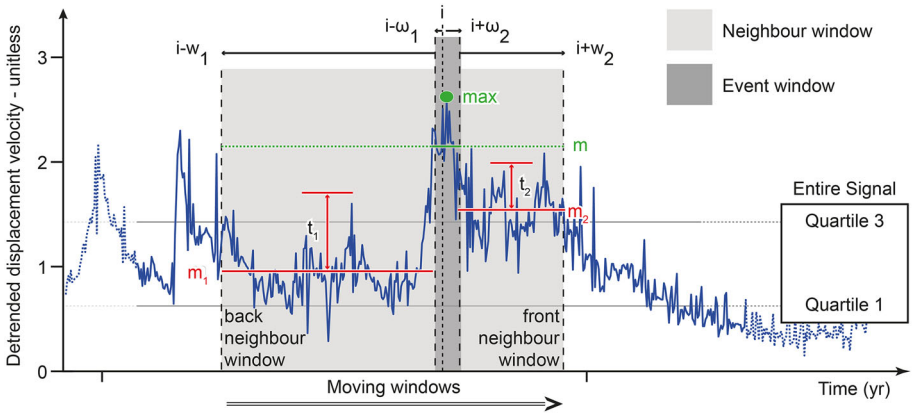

Fig. 3 Outline of the event detection method showing the two moving windows, a neighbor window separated in two parts (back and front) and an event window. This method needs the calibration of six parameters: 'safety' margin (t_1, t_2), neighbor window half-width (w_1, w_2), event window half-width (ω_1, ω_1). The scanning increment date is denoted by i

3.2 Detection of events

The method to detect LD or HD events is based on two moving windows scanning the displacement velocity time series (Fig. 3). The peak or trough characteristics (width and amplitude) are first taken into account in the detection process by a moving window named the *event window*. The characteristics of the background signal neighboring the considered event are defined by a second moving window named the *neighbor window*. This window consists in two parts (back part and front part) on either side of the event window. Since the patterns of the displacement velocity peaks and troughs are not symmetrical, both moving windows have the possibility to be asymmetrical with respect to the scanning increment date (Fig. 3). The neighbor window never overlaps with the event window. The detection, within a 10-day time interval, of peaks and troughs on all selected displacement velocity time series allows the definition of LD/HD events.

For a given displacement velocity time series, the condition for a displacement event to be considered as a HD event peak is threefold (Fig. 3). First, the mean value within the previously defined event window must be larger than the third quartile of the entire displacement velocity time series. Second, the mean value within the event window must be larger than the mean of the back part of the neighbor window to which a 'safety' margin is added. Third, the second condition also applies to the front part of the neighbor window, with a different safety margin value. Eventually, if the three above-mentioned conditions are fulfilled, then the date of the detected peak is defined as the date corresponding to the maximum value of displacement velocity within the event window (Fig. 3). The reverse procedure allows to detect a LD event trough: The mean value of the event window must be lower than the first quartile, and it must also be lower than the mean values of the back and front parts of the neighbor window, themselves lowered by 'safety' margins. Similarly, the date of the detected trough is defined as the date corresponding to the minimum value of displacement velocity within the event window.

A period of 20 days devoid of any LD/HD events is imposed after each identified LD/HD event, in order to reduce rainfall index information redundancy between successive events. This condition is required to improve the SVM classifier. Ideally, the LD/HD event-free period should be equal to the maximum number of days covered by the rainfall index (150 days in this study). However, by doing so, the amount of detected events will be significantly reduced, leading to a loss of statistical meaning of the rainfall threshold. A 20-day period is an acceptable trade-off. The event detection method requires 6 parameters to be estimated (Fig. 3): (i) back and front neighbor window widths (w_1, w_1), (ii) the event window widths on either side of the scanning increment date (ω_1, ω_1) and (iii) back and front 'safety' margins (t_1, t_2), (ii). These parameters are calibrated with an optimization algorithm.

3.3 Calibration of the parameters

A supervised learning method is implemented to calibrate the parameters of the event detection. This learning method uses a training interval where LD and HD events are identified manually on a set of selected displacement velocity time series. The training interval is a part of the whole study time interval. The event detection method parameters are adjusted on this training interval, with respect to manually identified events, with the use of an optimization algorithm. Once the method is calibrated, it is applied to the whole study time interval in order to define a list of LD and HD events required for the rainfall

index definition. Since this method mixes manual and automatic procedures, it is considered as a semiautomatic method.

An automatically identified event is considered as valid (true positive) if and only if it falls within a 10-day interval from a manually identified event. In the reverse case (more than 10 days), the automatically identified event is considered as a false positive. The optimization algorithm aims at minimizing the quantity $-\lambda_1 \mathrm{TPE} + \lambda_2 D_{\mathrm{avg}} + \lambda_3 \mathrm{FPE}$ which is composed of three terms: (i) TPE, the proportion of true-positive automatically identified events (Eq. 1), (ii) D_{avg}, the average deviation of the time difference between manually and automatically identified matching events (Eq. 2) and (iii) FPE, the proportion of false-positive automatically identified events (Eq. 3). A global optimization method, the simulated annealing (Kirkpatrick et al. 1983; Černý 1985), is used in the minimization process. The weighting factors λ_1, λ_2 and λ_3 are applied to each of the terms in order to balance their relative influence in the optimization process. The weighting factors are adjusted manually ($\lambda_1 = 1$, $\lambda_2 = 0.01$ and $\lambda_3 = 0.02$).

The six parameters of the event detection method are calibrated separately for LD and for HD events. In order to avoid unrealistic values, the calibration algorithm seeks the parameter values within predefined ranges: w_1 and w_2 ranging from 2 to 200, ω_1 and ω_1 ranging from 1 to 20 and t_1 and t_2 ranging from 0 to 4.

In summary:

$$\mathrm{TPE} = \frac{\mathrm{Nb_a}}{\mathrm{NbT_m}} \tag{1}$$

$$D_{\mathrm{avg}} = \frac{\sum_{i=1}^{\mathrm{Nb_a}} \left(\sqrt[2]{(D_{ai} - D_{\mathrm{m}i})^2} \right)}{\mathrm{Nb_a}} \tag{2}$$

$$\mathrm{FPE} = \frac{\mathrm{NbT_a} - \mathrm{Nb_a}}{\mathrm{NbT_a}} \tag{3}$$

with:

$\mathrm{NbT_a}, \mathrm{NbT_m}$ total number of events identified automatically or manually

$\mathrm{Nb_a}$ number of events automatically identified which match with manual events

$D_{\mathrm{a}}, D_{\mathrm{m}}$ date of automatic and manual events which match together.

4 Rainfall threshold definition method

The support vector machines (SVM) linear classifier is used to define an optimal and objective rainfall threshold by finding the best line separating two classes of n dimensions. A nonlinear classification can be achieved with the SVM classifier by using the so-called kernel trick. For the two-dimensional rainfall index, only the linear kernel is used, while for the multi-dimensional rainfall index, the linear kernel and the radial basis function kernel are tested. The SVM calibration and threshold performance are assessed with the cross-validation method by computing an average misclassification error rate (MER). The SVM analysis is performed with the multiplatform package LIB-SVM© (Chang and Lin 2011). The SVM classifier as well as the SVM classifier calibration and the kernel selection procedures are detailed in 'Appendix.'

4.1 The classical approach: the two-dimensional rainfall index (2DI)

Terlien (1998) showed the importance of selecting the proper period extent for the definition of a failure threshold. In several studies, the choice of the period extent of the antecedent rainfall is explored empirically, with no optimization to find the best number of days which maximizes the classification performance. In this study, the rainfall threshold is estimated for all combinations of antecedent and precedent periods varying from 2 to 150 days and from 1 to 10 days, respectively. The 150-day period is based on the study of Vallet et al. (2015a) which shows that the best coefficient of determination between the cumulative groundwater recharge and the landslide velocity is obtained for periods from 68 to 132 days. The impact of a rainfall event after a 150-day period therefore is considered as negligible.

The antecedent rainfall and the precedent rainfall match with the cumulated amount of rainfall over a specified number of days before an event (unstable or not). The precedent and the antecedent periods correspond to short and long periods, respectively (see Sect. 2.1 and Fig. 2a). The establishment of the threshold must be based on independent variables in order to be statistically true (Peruccacci et al. 2012). Consequently, the two periods, antecedent and precedent, do not overlap and are always adjacent. Groundwater hydrodynamic processes due to drainage are nonlinear, and an old rainfall event displays less impact than the most recent event on the aquifer saturation state (Canuti et al. 1985; Crozier 1986). As a consequence, a decay weight factor α is applied to the cumulated rainfall amount to take into account this nonlinearity (Eq. 4). Fifteen weighted sum combinations based on 5 decay factors α equal to 1, 0.99, 0.98, 0.95 and 0.90 are tested (Figs. 1 and 4).

For α being equal to one, the decreasing cumulated rainfall amount WI matches with a classical arithmetic sum.

$$\mathrm{WI} = \sum_{i=1}^{n} \alpha^{(i-1)} y(i) \tag{4}$$

where WI, decreasing cumulated rainfall amount of an event (mm); n, cumulative period extent (day); i, ith day ($i = 1$ match with event day); y, recharge or rainfall (mm); α_i, decay weight factor ($\alpha = 1$ for $i = 1$).

The two-dimensional rainfall index approach leads to 24,450 combinations which are evaluated with the SVM method. The SVM classifier performance (based on MER) is used to assess the best combination.

4.2 The new approach: the multi-dimensional rainfall index (MDI)

The maximum MDI dimension is set to 150 days that is the same as the maximum number of days allowed for the two-dimensional rainfall index (Fig. 2b). From a statistical point of view, it is important to find the most parsimonious model for the classification. It is well known that when the amount of data is moderate, a too complicated model can lead to poor prediction due to the lack of data available to estimate that model (Hastie 2009). This is known as the 'bias variance trade-off.' Furthermore, not all dimensions (also called features in this paper) are relevant in the event classification, i.e., the class labels can be predicted by only a few number (k) of features from the total available number p of features ($k \ll p$). In our case, the following question is a key question: How many days of

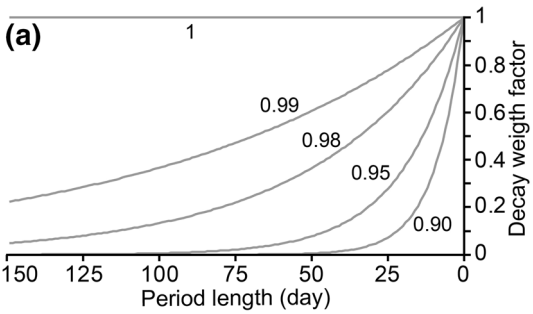

(b)

Combination	Decay weigth factor: Precedent period	Decay weigth factor: Antecedent period
1	1	1
2		0.99
3		0.98
4		0.95
5		0.90
6	0.99	0.99
7		0.98
8		0.95
9		0.90
10	0.98	0.98
11		0.95
12		0.90
13	0.95	0.95
14		0.90
15	0.90	0.90

Fig. 4 Determination of the rainfall index in the case of the two-dimensional approach with **a** plot of the 5 decay weight factors and **b** the set of 15 tested combinations coupling the 5 decay factors and the precedent and antecedent periods

precipitation/recharge are necessary to accurately predict whether an event is unstable or not?

Penalized SVM formulations (also called Least Absolute Shrinkage and Selection Operator or LASSO SVM penalty) were developed to seek sparse solutions by removal of irrelevant and redundant dimensions (Knight and Fu 2000; Hastie 2009). For this study, the penalized SVM classifier analysis is tested with the MATLAB© code NLPSVM (Fung and Mangasarian 2004), but the results, which consist in scattered selected features, are not consistent with hydrogeological processes. Instead, in order to seek the shorter continuous interval minimizing MER, a sensitivity analysis is carried out by iterating precipitation and recharge MDIs from 1 to 150 days (Fig. 1). For each iteration, a traditional SVM model is performed and the corresponding MER is computed. The MDI solution having the minimum MER is selected as the best solution to separate stable events from unstable events. Therefore, the multi-dimensional rainfall index approach leads to evaluate only 300 combinations.

4.3 Validation procedure to test the forecast ability of the rainfall threshold

Most rainfall threshold studies are conducted only by determining a threshold based on a list of discrete rainfall events, but do not test their operational applicability with a validation procedure performed against an independent continuous dataset recorded over a period different from the one used for the rainfall threshold definition (Martelloni et al.

2012; Bernardie et al. 2014). Landslide risk managers deal with continuously monitored rainfall datasets and also with weather forecasts. Even if a rainfall threshold defined with discrete historical stable/unstable events gives an acceptable classification performance, there is no guarantee that it can also give good classification performances on continuously monitored present-day or forecast rainfall datasets. In particular, it could lead to false positives or it could miss the detection of unstable events. In order to simulate hazard management requirements, the rainfall threshold forecast ability is tested against periods of high destabilization. These periods will be referred to as expected destabilization stages (EDS) which are arbitrarily defined as days during which the landslide velocity is larger than its third quartile. In other words, during EDS periods, the displacement velocity is greater than 75 % of its recorded values. The forecast ability is evaluated with a sensitivity analysis based on SVM probability outputs over an independent period. Two performance criteria are computed on the validation interval and plotted for each threshold solution: (i) the proportion of detected EDS (number of automatically detected true-positive unstable events divided by total number of EDS days) and (ii) the proportion of false-positive events (number of automatically detected false-positive unstable events divided by the total number of days of the independent validation time interval).

5 Geological and hydrogeological setting of the study area

The Séchilienne landslide is located to the southeast of Grenoble (France), on the right bank of the Romanche River on the southern slope of the Mont-Sec massif (Fig. 5). The landslide is located in the Belledonne crystalline belt and is composed of micaschists. The micaschists are characterized by a N–S trending vertical foliation. Carboniferous to Liassic sedimentary deposits unconformably cover the micaschists along the massif ridge line, above the unstable zone. Locally, glacio-fluvial deposits overlie both the micaschists and the sedimentary deposits.

The Séchilienne landslide is limited eastwards by a N–S fault scarp and northwards by a major head scarp of several hundred meters wide and tens of meters high below the Mont-

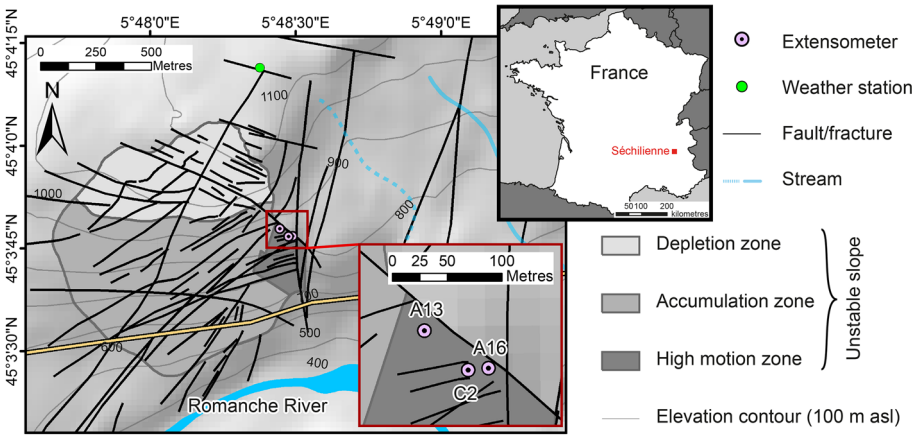

Fig. 5 Map of Séchilienne landslide with location of the monitoring network used in this study. Elevation is given in meters above sea level (m asl)

Sec. Rare geomorphological evidence allows to define precisely the western and southern boundaries of the unstable area. Below the head scarp, between 1100 and 950 m asl (above sea level), a low-slope depletion zone shows an area in depression, while between 950 and 450 m asl, the slope becomes steeper (>40°) and is interpreted as an accumulation area (Vengeon 1998; Le Roux et al. 2011). The slope is cut by a dense network of two sets of near-vertical open fractures trending N110° to N120° and N70°. The Séchilienne landslide is characterized by a deep progressive deformation controlled by the network of faults and fractures and by the absence of a well-defined basal sliding surface. The landslide is affected by a deeply rooted (about 100–150 m) toppling movement of the N50° to 70° slabs to the valley (accumulation zone) coupled with the sagging of the upper slope (depletion zone) beneath the Mont-Sec (Vengeon 1998; Durville et al. 2009; Lebrouc et al. 2013). The displacement monitoring shows displacement velocity vectors being relatively homogeneous in direction (N140°) and in dip angles (10° to 20° toward the valley). Low displacement velocities (2–15 cm/yr) are observed for both the depletion and the accumulation zones (Le Roux et al. 2011). These velocities gradually decrease toward the west and the south, allowing to estimate the limits of the unstable area. A very actively moving zone with high displacement velocities about 150 cm/yr is distinguishable from the unstable slope.

5.1 Hydrogeology and rainfall triggering

The hydraulic conductivity of the Séchilienne is higher than that of the underlying stable bedrock (Vengeon 1998; Meric et al. 2005; Le Roux et al. 2011), thus leading to a landslide perched aquifer (Guglielmi et al. 2002). The fractured metamorphic bedrock beneath the landslide contains a deep saturated zone at the base of the slope and an overlying thick (about 100 m) vadose zone. The recharge of the landslide perched aquifer is essentially local, enhanced by trenches and counterscarps which tend to limit the runoff and to facilitate groundwater infiltration (Vallet et al. 2015b). However, the hydrochemical analyses of Guglielmi et al. (2002) show that the sedimentary deposits distributed above the landslide hold a perched aquifer which can recharge the landslide perched aquifer. The groundwater flow of the entire massif is mainly controlled by the well-developed network of fractures with high flow velocities [up to a few kilometre per day; (Vallet et al. 2015b)]. The triggering of the Séchilienne landslide is likely driven by a two-layer hydrosystem consisting of a landslide perched aquifer and a deep aquifer over the whole massif hosting the landslide (Cappa et al. 2014; Vallet et al. 2015c). As a result, the Séchilienne landslide is characterized by a good correlation between precipitations and displacement velocities (Rochet et al. 1994; Alfonsi 1997; Durville et al. 2009; Chanut et al. 2013). Vallet et al. (2015a) show that the Séchilienne displacement rates are better correlated with the recharge than with the precipitation, reinforcing the significant role of groundwater flow in the Séchilienne destabilization.

5.2 Monitoring network and method implementation

The Séchilienne landslide is monitored by numerous displacement stations using a wide range of techniques (extensometer, radar, infrared geodesy, inclinometer, GPS). A weather station is located at Mont-Sec, a few hundred meters above the top of the disturbed zone (Fig. 5). This weather station is equipped with rain and snow gauges. The snow gauge provides an estimate of the snowpack thickness expressed in water depth. The equivalence between the snowpack thickness and the water depth is estimated with the measurement of

the attenuation of the cosmic radiation by the snowpack. Therefore, this station allows to account for snow storage and melting which cause infiltration at different rates and with different time delays between rain and snow. As a consequence, hereafter, precipitation will combine rainfall and snow melt as single component.

Displacement and weather data are recorded at a daily rate. The daily displacement, identical to a velocity measurement in mm/day, is hereafter named displacement. The weather station is equipped with rain and snow gauges. Extensometer stations are selected for displacement data as they are the most reliable displacement recording devices on the site and also because they have been operating since the very beginning of displacement monitoring. For the semiautomatic detection event method, three extensometers: A13, A16 and C2, are selected. They are located on the most active moving zone, which is also the most reactive zone with regard to precipitation events (Fig. 5). The event detection method is calibrated on the testing interval from January 1, 2001, to December 31, 2004 (about 20 % of the studied period), as displacement time series variations are representative of the overall time series for this period, and is then applied on the period from January 1, 1994, to December 31, 2011. The two rainfall threshold approaches are trained from January 1, 1994, to December 31, 2011 (same as for the event detection process interval), while the validation procedure is implemented over the recent period, from January 1, 2012, to August 31, 2013. The training interval, which is longer than the test interval, is constrained by SVM classification accuracy which is enhanced with the number of LD/HD events identified. For the validation procedure, the SVM classifications are filtered, with isolated detected one-day LD or HD events disregarded since not being significant enough to lead to a destabilization event. The currently existing Séchilienne warning system, partly based on precipitation, in addition to displacement rate, micro-seismic and rockfall monitoring, integrates an operational rainfall threshold (SWS threshold) defined as 80 mm of accumulated precipitation for a period of less than 3 days.

5.3 Recharge estimation

Evapotranspiration is estimated from temperature records by using the Penman–Monteith reduced-set equation (Allen et al. 1998) and Bristow–Campbell radiation equation (Bristow and Campbell 1984), calibrated against the benchmark Penman–Monteith equation (Allen et al. 1998) and radiation measurements, respectively. Calibration is performed with three neighboring weather stations, where all required parameters (temperature, wind, humidity and radiation) are measured. A soil water balance method is used to compute recharge with soil available water storage set at 105 mm and a runoff coefficient of 11 %. Information and details on the methodology adopted in this study can be found in Vallet et al. (2015a).

5.4 Displacement detrending

The long-term displacement records of the three extensometers show that displacement rates and amplitudes exponentially increased through time (Fig. 6b). The precipitation data series does not show any trend over the year, meaning that the displacement trend is independent of the recharge amount (Fig. 6a). Consequently for the same amount of precipitation, the Séchilienne displacement rate and magnitude responses increase steadily with time. The observed trend is the consequence of a progressive damaging of landslide mechanical properties due to long-term repetitive stresses which cause permanent deformation. This deformation can be assimilated to long-term creep (Brückl 2001; Bonzanigo

et al. 2007) and can lead to a decrease in the slope shear strength and/or to a modification of hydraulic properties (Rutqvist and Stephansson 2003). In addition to the trend, the Séchilienne landslide is constantly moving and shows large daily to seasonal variations. These variations are clearly linked to the recharge amount (Vallet et al. 2015c). Consequently, the semiautomatic event detection and the determination of EDS periods are based on the detrended displacement time series which is the true response of the landslide to the precipitation trigger.

The exponential trend is removed with the statistical multiplicative method ($y_t = T_t S_t I_t$) where the time series (y_t) is composed of three components (Madsen 2007; Cowpertwait and Metcalfe 2009; Aragon 2011): trend (T_t), seasonal (S_t) and irregular (I_t). In this study, the irregular and seasonal components are assumed to be linked to the precipitation triggering factor ($y_t = T_t R_t$ with $R_t = S_t I_t$). The trend is determined by curve fitting of a fifth-order polynomial (parametric detrending). The result is a detrended unitless time series (R_t) with both variance and mean trend removed. The time series decomposition process is illustrated with the A13 extensometer in the Fig. 6c.

6 Results

6.1 Semiautomatic event detection

The results of the semiautomatic event detection results are plotted in the Fig. 7, and the calibrated parameters are presented in Table 1. Over the training interval (January 1, 2001, to December 31, 2004), all the manually identified HD events are located in winter–spring seasons (high flow periods), whereas LD events take up the rest of the year. For HD events, 13 events are automatically detected among the 13 manually identified (100 %) and 0 false positive is identified (Fig. 7a). For LD events, 10 events are automatically detected among

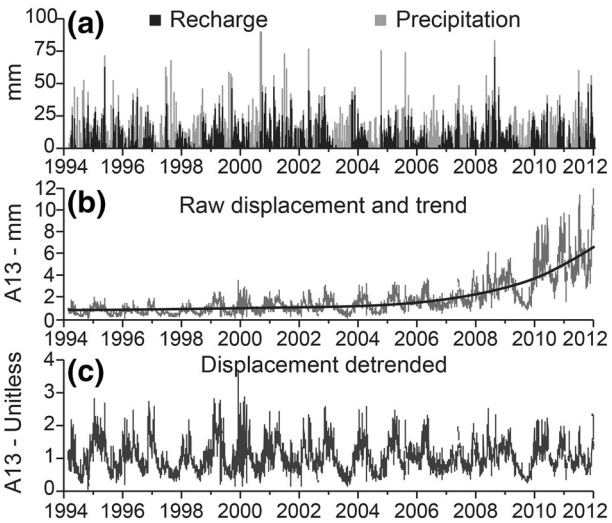

Fig. 6 Meteorological dataset and detrending of extensometer A13 records. **a** Precipitation and recharge dataset. **b** A13 daily displacement and parametric trend. **c** Detrended A13 daily displacement

the 13 manually identified (77 %), and 3 false positives are identified (Table 1 and Fig. 7a). The calibration performance is better for HD events, as peak patterns are better constrained (sharp width, large amplitude, short wave length, one HD event per peak), while several LD events can be identified within the same trough (longer wave length).

Fifty-seven HD events and 55 LD events are identified for the whole studied interval (January 1, 1994, to December 31, 2011) on the three detrended displacement time series and are plotted on the raw displacement time series (Fig. 7b). Detections of events are regularly spread over the time series interval, although only a few events are identified for some years (1997, 1999, 2003 and 2006). LD and HD events mainly occur in summer–autumn and winter–spring, respectively, reflecting the seasonal pattern of manual events.

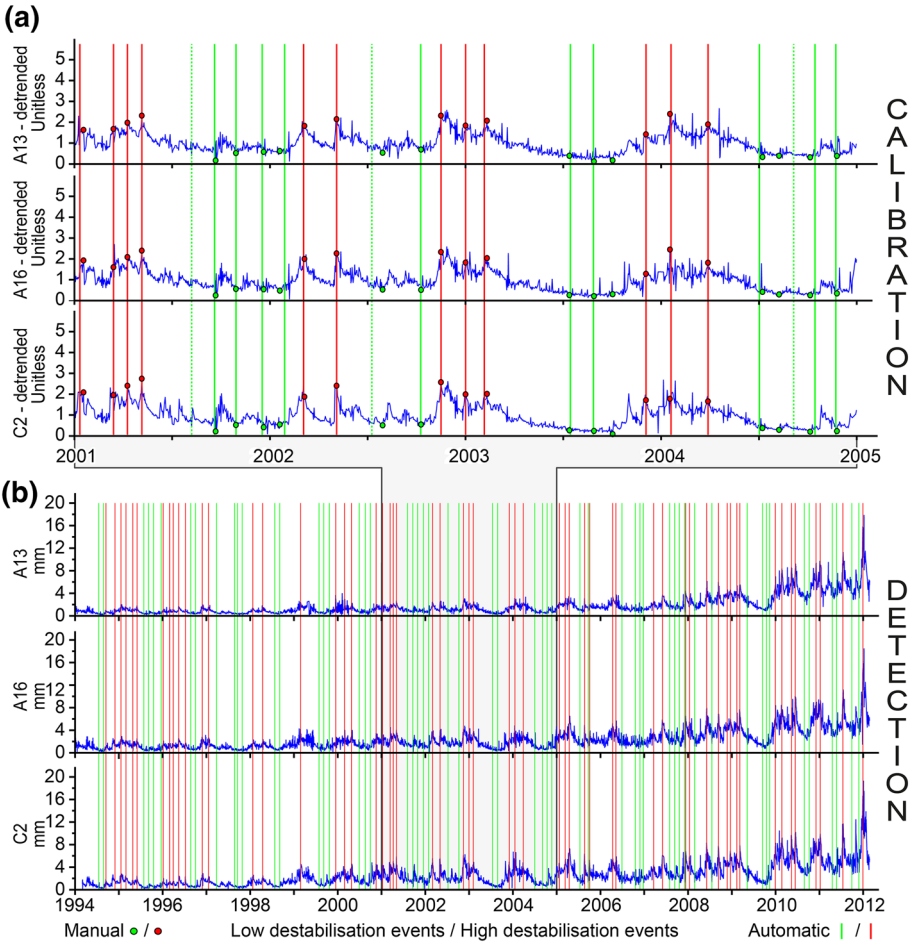

Fig. 7 Results of the semiautomatic event detection method for the A13, A16 and C2 extensometers. **a** Calibration results of the method with manual and automatic events detected relatively to detrended daily displacement. **b** Processing results of the calibrated method relatively to raw daily displacement on the whole studied interval. *Dashed lines* stand for automatic false-positive events relatively to the manually identified events

Table 1 Results of the calibration of the automatic event detection method for low-destabilization (LD) events and high-destabilization (HD) events

Type		LD event	HD event
Calibrated parameters	Neighbor window (w_1, w_2) [day]	(123; 56)	(80; 16)
	Event window (ω_1, ω_2) [day]	(2; 3)	(2; 2)
	'Safety' margin: (t_1, t_2) [mm]	(0.0154; 0.0095)	(0.0524; 0.0649)
Performance	True-positive events (TPE) [%]	77	100
	Average date deviation (D_{avg}) [day]	3.5	1.33
	False-positive events (FPE) [%]	23	0

The number of identified events is well balanced for each class, and the total number of events is sufficient to perform a SVM analysis.

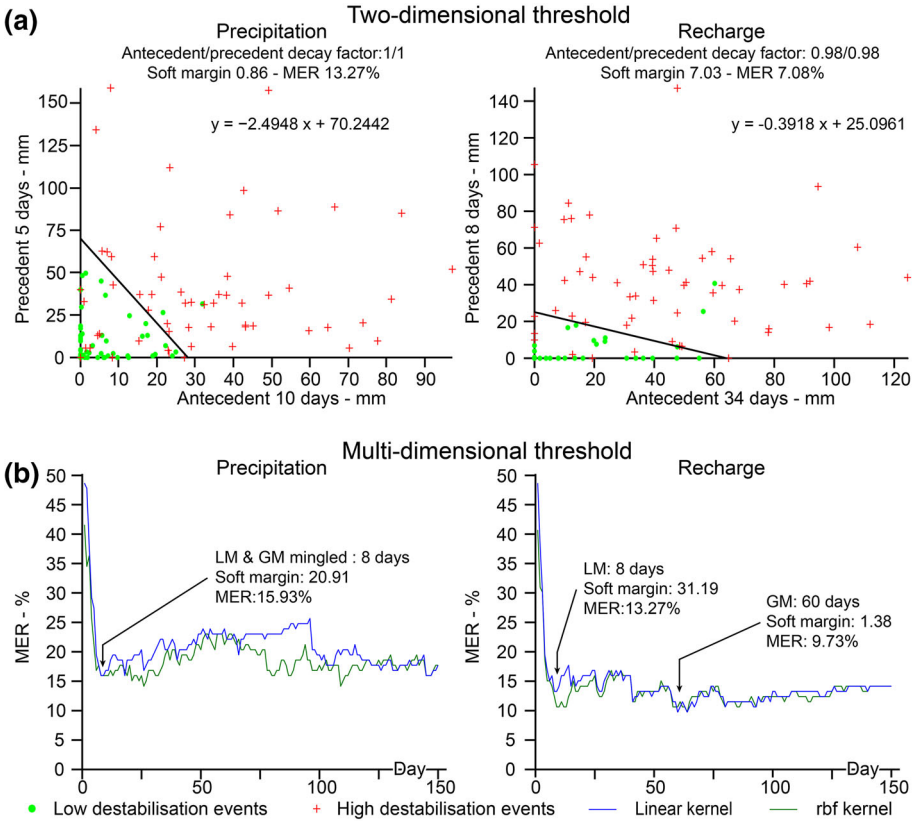

Fig. 8 Results of rainfall threshold classification on the training interval for the **a** two-dimensional and **b** multi-dimensional approaches. MER, LM and GM stand, respectively, for misclassification error rate, local minimum and global minimum

6.2 Rainfall threshold performances on the training interval

Among the combinations tested for the two-dimensional threshold (2DI threshold), the best rainfall threshold MER for precipitation (13.27 %) is about two times larger than the best MER obtained with recharge (7.08 %, Fig. 8a). The antecedent precipitation/precedent precipitation indexes involved in the two best threshold performance are 10/5 days for precipitation (short-term) and 34/8 days for recharge (long-term) with decay weight factors of 1 and 0.98 (identical for the two periods for the two cases), respectively.

Regarding the multi-dimensional approach (MDI rainfall threshold), the two tested kernels (linear and RBF) show no significant differences in the MER performance for precipitation as well as for recharge (Fig. 8b). The linear kernel, which is much simpler than the RBF kernel, is chosen to determine the MDI rainfall threshold. The MDI number of days, from which MER is not significantly improved, is identified as a local minimum, whereas the MDI number of days having the minimum of MER is identified as a global minimum. Regarding precipitation, the local and the global MER minima are mingled (MER 15.93 %) for a rainfall MDI of 8 days. Regarding recharge, the local minimum (MER 13.27 %) is obtained at 8 days, whereas the global minimum (MER 9.73 %) is obtained at 60 days, both recharge MERs being lower than the MER derived from precipitation.

Both threshold approaches lead to short-term and long-term components. Recent studies (Guglielmi et al. 2002; Cappa et al. 2014) show that a two-layer hydrosystem may destabilize the Séchilienne landslide, with a shallow perched aquifer localized in the unstable area and a deep aquifer below the landslide. The perched aquifer behavior is more reactive to short-term precipitation events, whereas the deeper aquifer is more sensitive to long-term seasonal recharge variations. In order to take into account the possible coupling of the two aquifers on the landslide destabilization, a rainfall threshold is estimated for each threshold approach by averaging the probability of the short- and long-term components (the so-called composite threshold). The two-dimensional precipitation and recharge thresholds are combined, while for the multi-dimensional threshold, only the recharge short-term and long-term MDI solutions are used. Although the precipitation is a more appropriate signal to characterize the landslide perched aquifer, the short-term component of the recharge is chosen for the multi-dimensional threshold. Indeed, the precipitation and recharge short-term optimal solutions of the multi-dimensional threshold occur within the 8th dimension, but recharge shows a slightly enhanced MER (see Sect. 7.2 for process explanation). In the case of the composite threshold, if infra-day (e.g., hourly) precipitation dataset were available (which is not the case for Séchilienne), it would worth testing this dataset to check whether the performances of precipitation threshold accounting for the landslide perched aquifer are improved or not.

6.3 Rainfall threshold performances on the forecast testing interval

The performances and the results of the thresholds estimated with the 2DI and the MDI approaches on the forecasting testing interval are plotted *versus* the time in Fig. 9. Figure 10 shows the performances of these thresholds according to the threshold SVM probability outputs.

The probability output signals show similar patterns between respective components of 2DI threshold and MDI threshold approaches, i.e., short term, long term and composite (Fig. 9b, c). For the SVM default classification (probability $\geq$0.5), regardless of the

approach, short-term components show a more scattered HD event detection, sensitive to precipitation events, with several false positives during low flow periods. Conversely, the long-term components show a more continuous HD event period during high flow periods, also leading to several false positives. The two-dimensional approach is characterized by a

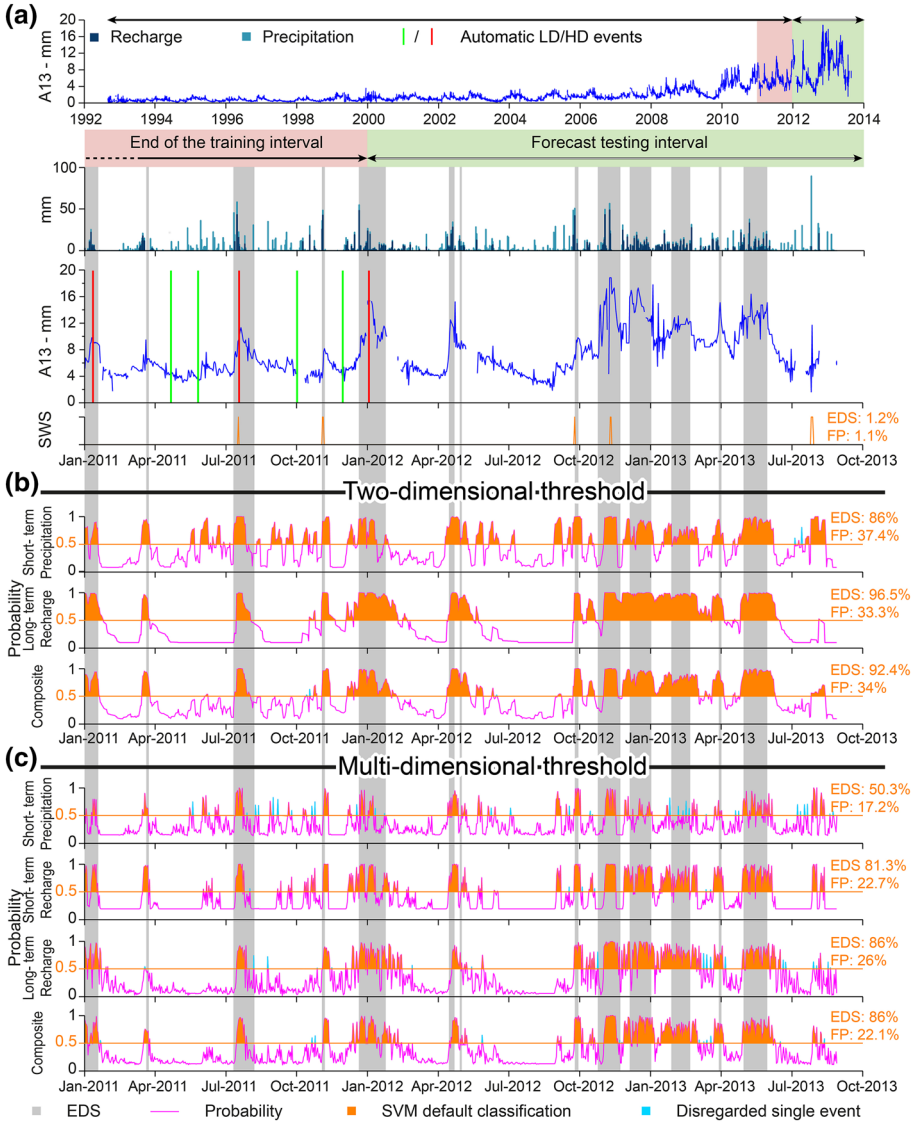

Fig. 9 Results of rainfall threshold classification on the forecast testing interval **a** A13 raw daily displacement and precipitation/recharge with the LD and HD automatic events. **b** Two-dimensional and **c** multi-dimensional threshold approaches. The short- and long-term components as well as the resulting composite threshold are displayed for both approaches. For each component, the probability outputs and the SVM classification performances for probability ≥ 0.5 are plotted. Performance indicators are the proportion of EDS detected (EDS) and the proportion of false positives (FP). EDS, LD and HD stand for expected destabilization stages, low-destabilization events and high-destabilization events

less noisy probability signal, which can be explained by the decreasing sum acting a smoothing function (Fig. 9b). The SWS threshold shows a low performance with an EDS detection at 1 %.

For the 2DI and MDI approaches, the rainfall thresholds estimated with precipitation are always outperformed by those estimated from recharge, whatever the probability limits (Fig. 10). The composite 2DI threshold does not improve the classification performance, and the recharge 2DI threshold is clearly the best solution of the classical two-dimensional approach (Figs. 9b and 10a). On the contrary, the composite MDI threshold slightly improves the classification performance, compared to the short-term and long-term components of the recharge MDI threshold, mostly for false positives in a proportion lower than 15 % (Figs. 9c and 10b).

7 Discussion on the event detection method and the rainfall threshold performances on the forecast testing interval

7.1 Event detection

The event detection method shows a very good performance and produces a large number of events to train SVM classification. Although the method is relatively robust and easy to implement, it requires a wide data interval with at least a daily time step to produce a sufficient number of events (statistical significance) for rainfall threshold classification. However, improvements in instrumental technology allow more and more cost-effective monitoring, and nowadays, many landslides have been monitored daily for more than 10 years. In addition, more and more landslide monitoring data are available with the open-access initiatives of the scientific community, such as the French OMIV observatory

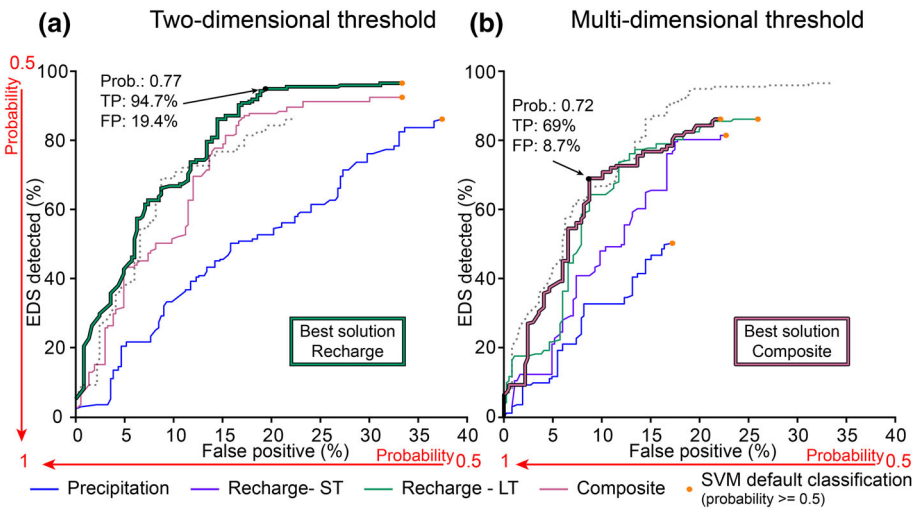

Fig. 10 Rainfall threshold performance comparison with proportion of false positives and EDS detected on the forecast testing interval for **a** the two-dimensional approach and **b** the multi-dimensional approach. EDS stand for expected destabilization stages. TP and FP stand for true positive (i.e., EDS detected) and false positive. ST and LT stand for short term and long term

(Multidisciplinary Observatory of Versant Instabilities) in charge of the Séchilienne landslide. The proposed event identification should therefore be suitable for a large number of landslides, and this number is expected to increase over the years.

7.2 Precipitation, recharge and composite rainfall threshold

Regardless of the approach (2DI or MDI), the recharge thresholds show the best performances. The use of precipitation leads to a poor performance/error ratio and is likely to produce an unreliable rainfall threshold. In addition, the best precipitation 2DI threshold does not require a decay factor in the decreasing cumulated precipitation amount computation (Fig. 8a), meaning that the short-term component does not involve a nonlinear relationship with the displacement records. This reflects the fact that the key parameter to account for destabilization of deep-seated landslides controlled by nonlinear groundwater processes is not precipitation but recharge (Van Asch et al. 1999; Vallet et al. 2015a).

The composite threshold shows the best performance for the MDI approach, whereas the recharge threshold shows the best performance for the 2DI approach (Fig. 10). This difference can be explained by the fact that the composite MDI threshold is estimated only with the recharge component, whereas the composite 2DI threshold involves the precipitation component. The rainfall threshold takes only interest in classifying extremely low- or high-destabilization events resulting from extremely high or low precipitation events. Consequently, the soil–water balance which acts as a filter by removing numerous precipitation events of low magnitude (soil water storage cutoff) enables to define a better rainfall threshold identifying less false positives. This is another advantage to use the recharge signal rather than the precipitation signal. Lastly, the good performance of the composite threshold agrees with a landslide destabilization triggered by a two-layer hydrosystem.

7.3 Two-dimensional versus multi-dimensional rainfall threshold

The similarity of the probability output signals between the two methods (2DI and MDI) indicates that the weight applied by the SVM classifier to the dimensions of the MDI successfully reproduces the nonlinear relationship between precipitation/recharge input and landslide destabilization (Fig. 9). Unlike the 2DI rainfall threshold determination, there is no need to introduce parameters such as decay factors in order to adjust for the nonlinearity. The multi-dimensional approach (MDI) fulfills the requirement of the method to adhere to the concept of requisite simplicity (Stirzaker et al. 2010), balancing technical accuracy with utility for operational implementation. For all these reasons, although the 2DI threshold globally shows slightly better performance, a composite MDI threshold is an efficient alternative method. Indeed, it has the benefit of having a truly objective and cost-effective computation method. From an implementation point of view, although the two-dimensional approach requires numerous hypotheses and extended computation time, it has, nevertheless, the advantage of defining the rainfall threshold by a simple linear equation which can be used regardless of the SVM model from which it originates (Fig. 8a). Conversely, the MDI rainfall threshold method does not require any hypothesis or extended computation time. It, however, requires the use of the SVM established model to discriminate between events.

7.4 Relevancy of the SVM probability output

The SVM probability outputs are investigated in Fig. 10 with a sensitivity analysis in relation to the proportion of detected EDS and false-positive events. Whatever the approach (2DI and MDI), the probability outputs allow a finer and more flexible classification than the SVM default classification (probability $\geq$0.5). In the case of the recharge 2DI threshold (Fig. 10a), the default SVM classification identifies 33.3 % of false-positive events for a 96.5 % proportion of detected EDS. The modification of the probability limit to 0.77 allows, for a similar proportion (94.7 %) of detected EDS, to decrease the proportion of false-positive events to 19.4 %, that is an improvement of about 40 %. The sensitivity analysis shows that the higher the probability, the fewer the EDS events detected and the fewer the false-positive events (Fig. 10).

For each rainfall threshold, the break point on the detected EDS *vs.* false-positive plot above which the EDS proportions do not significantly increase compared to the false-positive proportion has been identified (highlighted by arrows in Fig. 10). This point corresponds to the probability limit which maximizes the proportion of detected EDS with respect to the proportion of false-positive events.

The composite MDI threshold probability outputs and the A13 displacement time series are plotted for seven limits from 0.5 to 0.99 for illustration purposes (Fig. 11). These results highlight the relevance of using a validation procedure, in order to assess the forecast ability of the rainfall threshold (Martelloni et al. 2012; Bernardie et al. 2014). Indeed, the validation procedure allows to choose the appropriate probability limit

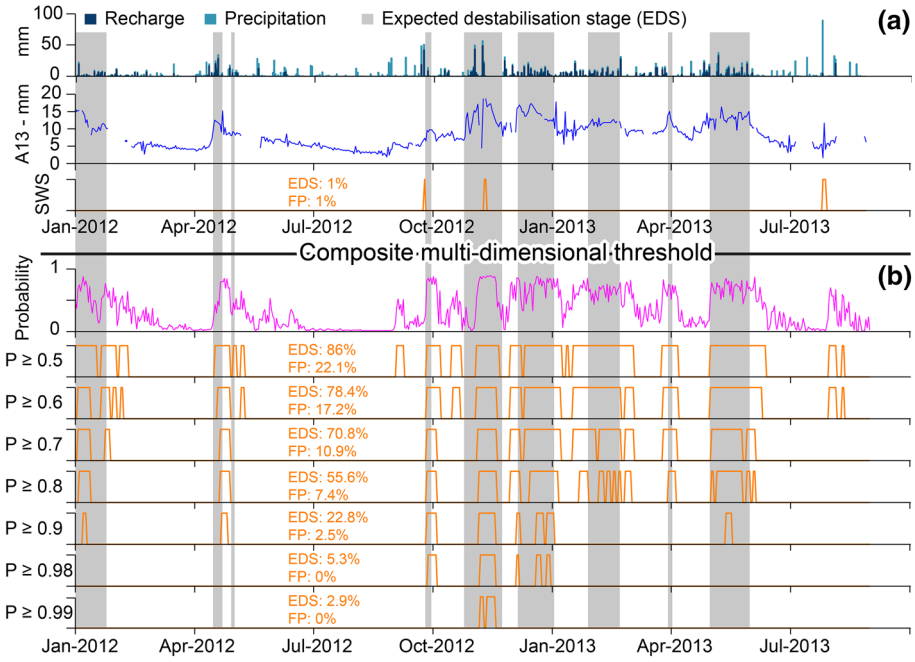

Fig. 11 Illustration of probability output versatility from the composite multi-dimensional threshold. **a** A13 raw daily displacement and precipitation/recharge. **b** Seven different limits corresponding to increasing probabilities from 0.5 to 0.99 associated with the proportion of expected destabilization stages (EDS) detected and of false positives (FP)

according to the threshold purpose and to assess whether the accuracy of the threshold is sufficient to be integrated or not into a warning system. Time series signal patterns of displacement and SVM probability outputs (Figs. 9 and 11) suggest that the SVM probability outputs might be linked to hydraulic stress levels triggering the landslide destabilization, but this has still to be proven.

7.5 Operational applicability of the rainfall threshold in the Séchilienne warning system

The low performance of the present-day SWS threshold can be partly explained by the fact that the identified periods for EDS do not match the detection requirement of the rainfall threshold in the Séchilienne warning system. However, the SWS threshold misses numerous high-destabilization events, demonstrating that the SWS threshold does not consistently link rainfall input with landslide destabilization (Fig. 9). The composite MDI threshold outperforms the presently used SWS threshold whose probability output flexibility makes it suitable to be integrated in the Séchilienne warning system (Fig. 11).

8 Conclusion and perspectives

The aim of this study is to develop a new operational objective method to determine statistical rainfall thresholds for deep-seated landslides. Combining the SVM multi-dimensional rainfall threshold with a semiautomatic event detection method produces very good results and constitutes an appropriate tool to define an objective and optimal rainfall threshold. In addition to shortened computation times, to the non-necessity of pre-requisite hypotheses and to a fully automatic implementation, the newly introduced multi-dimensional (MDI) approach shows performances similar to the classical two-dimensional approach. This shows its relevance and its suitability for defining a rainfall threshold. Moreover, the multi-dimensional approach allows to find the best period combination which maximizes the separation of stable and unstable events. Lastly, this study shows that the recharge is a relevant parameter to be taken into account for deep-seated rainfall-induced landslides. Using the recharge rather than the precipitation significantly improves the delineation of a rainfall threshold separating stable and unstable events. The performance and accuracy of the multi-dimensional composite threshold make it an appropriate method for integration in the Séchilienne landslide warning system. Probability outputs allow to design an adjustable rainfall threshold adapted to early warning system requirements, especially for those having multi-step crisis alerts.

The outcomes of these results are numerous. It would worth testing the proposed method for other deep-seated or shallow landslides in order to evaluate its application and performances. As well, it would worth comparing performances of the proposed method to frequentist and Bayesian studies. Indeed, the intensity–duration thresholds, especially for the identification of the triggering rainfall conditions (Segoni et al. 2014), are often defined by resorting to subjective decisions. For shallow landslides, it may be necessary to adjust the method by defining a multi-dimensional index at an infra-hourly time step, in order to characterize intensity and duration of rainfall events. Another application would be to define a rainfall threshold with the proposed method for micro-seismic and rockfall events, linked to landslide destabilization mechanisms. Lastly, in order to improve threshold

accuracy, it will be of interest to evaluate rainfall threshold biases induced by meteorological forecast uncertainties.

Acknowledgments This research was funded by the program SLAMS (Séchilienne Land movement: Multidisciplinary Studies) of the Agence Nationale de la Recherche. The meteorological and displacement data were supplied by CEREMA Lyon. The authors acknowledge the support of Jean-Pierre Duranthon and Marie-Aurélie Chanut from the CEREMA Lyon. Lastly, the authors thank the editor and the two anonymous referees for their constructive comments.

Appendix: Application of the support vector machines for the determination of rainfall threshold

The SVM classifier tool

The support vector machines (SVM) method is a widely used two-class linear classifier, belonging to supervised learning models and kernel methods (Hastie 2009). The purpose of a supervised learning method is to produce an inferred function from a set of training data (with known properties). The inferred function is then used to classify new data for prediction. The SVM classifier can be used to find the best hyperplane separating two classes of n dimensions by maximizing the margin between the two classes (Fig. 12). The margin can be defined as the width between data points (called support vectors) of the two classes that are closest to the separating hyperplane with no points within the margin (Cristianini 2000). Data scaling or normalization are strongly recommended to enhance the SVM classifier performance (Hsu et al. 2003; Ben-Hur and Weston 2010). For this study, all data are scaled to the [0, 1] range.

The SVM classifier assumes that the data are linearly separable and requires that the best hyperplane classifies each point correctly. However, a rainfall threshold classification presents possible nonlinear separable data. In order to achieve a larger margin, the soft margin SVM formulation (Cortes and Vapnik 1995) allows some points to be in the margin or even to be misclassified. This is achieved by introducing slack variables ε_i in the minimization program (Eq. 5). A soft margin cost parameter C must be specified by the user. The C parameter controls the trade-off between errors of the SVM on training data and the margin maximization. Small values of C will produce a classifier with larger margins and will allow a higher proportion of misclassified sample data. The optimal hyperplane is obtained by solving the optimization problem in Eq. (5). The optimization function is built-in for the SVM packages used. More details and an introduction to the SVM classifier can be found in Hsu et al. (2003) and Ben-Hur and Weston (2010).

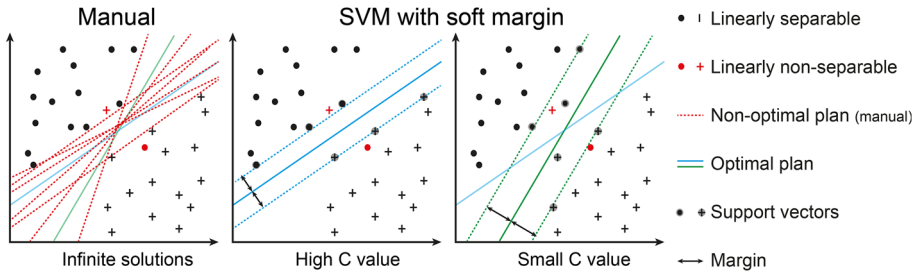

Fig. 12 Schematic illustration of the SVM classifier principle and the soft margin formulation

$$\begin{aligned} &\underset{w,b,\varepsilon}{\text{minimize}}\,\frac{1}{2}\|w\|^2+C\sum_{i=1}^{n}\varepsilon_i \quad \text{with} \quad \|w\|^2=\sum_{j=1}^{p}w_j^2 \\ &\text{subject to } y_i\left(w^T x_i+b\right)\geq 1-\varepsilon_i, \varepsilon_i \geq 0 \end{aligned} \tag{5}$$

with: w, normal vector of the classifier; p, number of dimensions; b, intercept of the separating hyperplane (also called bias); C, soft margin cost; y_i, labels $+1$ or -1; x_i, ith sample dataset (p-dimensional row); ε_i, slack variable; n, number of sample (observations).

SVM kernel selection

The efficiency of the SVM classification depends on the soft margin parameter, the selected kernel function and kernel parameters. The kernel function allows to map data from the input space to a higher-dimensional space where the SVM classifier can find a linear separating hyperplane (kernel trick). A nonlinear kernel can handle the cases for which the separation between class labels is nonlinear in the input space. In order to do so, the nonlinear kernel finds a linear solution in the feature space. In this study, the kernel is selected from the four commonly used kernel functions: linear, polynomial, radial basis function (RBF) and sigmoid.

Two-dimensional rainfall index

Although the RBF kernel is recommended by default for classification with a number of instances larger than the number of features (Hsu et al. 2003), the linear kernel is selected for the classical rainfall threshold. The choice of the linear kernel is justified as the nonlinearity is already taken into account by the decreasing cumulated rainfall amount. In addition, the linear kernel does not require the input of any parameter, so only the soft margin parameter (C) need to be adjusted. This allows a cost-effectiveness computation given the large amount (24,450) of combinations to explore.

Multi-dimensional rainfall index

For the multi-dimensional approach, the number of features involved in the classification varies from 1 to 150, whereas the number of instances (events) is constant. The linear and RBF kernels are tested and compared for each iteration. The linear kernel is selected for its cost-effectiveness and simplicity in calibration computation. Among the nonlinear kernels, the RBF kernel (Eq. 6) is chosen for the reasons mentioned by Hsu et al. (2003) and Ben-Hur and Weston (2010): having only one parameter γ to calibrate, generally outperforms other nonlinear kernels and presents less numerical difficulties.

$$K\left(X_i X_j\right)=\exp\left(-\gamma X_i X_j^2\right), \quad \gamma>0 \tag{6}$$

SVM calibration and threshold performance: cross-validation

The cross-validation is a statistical method which evaluates a model performance and is especially adapted to a learning predictive model such as the SVM classifier (Hsu et al. 2003; Refaeilzadeh et al. 2009; Ben-Hur and Weston 2010). The cross-validation consists in successive rounds where the dataset is randomly partitioned into two subsets: One will

be used for training the model (learning) with known properties, and the other will be used for validating the model with unknown properties (testing). The method ensures that all data are used both for training and validation. The cross-validation assesses the accuracy of the model to predict new data by estimating the average misclassification error rate (MER). The cross-validation is recommended for SVM calibration. It can also avoid model overfitting (Hsu et al. 2003). There are several methods to partition the data according to the goals of the study. In this study, a 'leave-one-out' cross-validation is chosen as it allows unbiased performance estimation. The leave-one-out is a particular case of k-folds cross-validation where k equals the number of observations. The k-folds method consists of dividing the dataset into k equal subsets (folds). Each fold in turn is used for validation, while the remaining $k-1$-folds are used for SVM training for k iterations.

The built-in MATLAB® function *fminsearch*, which is an unconstrained nonlinear optimization, is used to search for the best soft margin cost parameter C and the RBF parameter γ which minimizes MER of the cross-validation (calibration process). Because *fminsearch* is dependent on an initial estimate of the parameter to calibrate, an exponential grid search of C solutions from -4 to 8 (with an increment of 0.01 rounds) is performed for each SVM model. The *fminsearch* function is then applied to the model with the best performance. The calibration is performed for each tested combination. The MER obtained after SVM calibration from the leave-one out cross-validation is used to assess the classification performance for each tested combination for both the classical and new approaches. The MER is the ratio between the number of erroneous predictions and the total number of predictions produced.

References

Aleotti P (2004) A warning system for rainfall-induced shallow failures. Eng Geol 73:247–265. doi:10.1016/j.enggeo.2004.01.007

Aleotti P, Chowdhury R (1999) Landslide hazard assessment: summary review and new perspectives. Bull Eng Geol Env 58:21–44. doi:10.1007/s100640050066

Alfonsi P (1997) Relation entre les paramètres hydrologiques et la vitesse dans les glissements de terrains. Exemples de La Clapière et de Séchilienne. Rev Fr Géotech 79:3–12

Allen RE, Pereira LS, Raes D, Smith M (1998) Crop evapotranspiration: guidelines for computing crop water requirements, FAO Irrigation and drainage paper 56. Food and Agriculture Organization of the United Nations, Rome

Aragon Y (2011) Séries temporelles avec R: Méthodes et cas, Édition: Reprint. Springer Editions, Paris

Ben-Hur A, Weston J (2010) A User's guide to support vector machines. In: Carugo O, Eisenhaber F (eds) Data mining techniques for the life sciences. Humana Press, New York, pp 223–239

Ben-Yacoub S (1999) Multi-modal data fusion for person authentication using SVM. In: Proceedings of 2nd international conference on audio and video based person authentication. Washington, D.C., pp. 25–30

Bernardie S, Desramaut N, Malet J-P, et al (2014) Prediction of changes in landslide rates induced by rainfall. Landslides 1–14. doi: 10.1007/s10346-014-0495-8

Berti M, Martina MLV, Franceschini S et al (2012) Probabilistic rainfall thresholds for landslide occurrence using a Bayesian approach. J Geophys Res Earth Surf. doi:10.1029/2012JF002367

Binet S, Guglielmi Y, Bertrand C, Mudry J (2007) Unstable rock slope hydrogeology: insights from the large-scale study of western Argentera-Mercantour hillslopes (South-East France). Bulletin de la Société Géologique de France 178:159–168. doi:10.2113/gssgfbull.178.2.159

Bogaard T, Guglielmi Y, Marc V et al (2007) Hydrogeochemistry in landslide research: a review. Bulletin de la Société Géologique de France 178:113–126. doi:10.2113/gssgfbull.178.2.113

Bonzanigo L, Eberhardt E, Loew S (2007) Long-term investigation of a deep-seated creeping landslide in crystalline rock. Part I. Geological and hydromechanical factors controlling the Campo Vallemaggia landslide. Can Geotech J 44:1157–1180. doi:10.1139/T07-043

Bristow KL, Campbell GS (1984) On the relationship between incoming solar radiation and daily maximum and minimum temperature. Agric For Meteorol 31:159–166. doi:10.1016/0168-1923(84)90017-0

Brückl EP (2001) Cause-effect models of large landslides. Nat Hazards 23:291–314. doi:10.1023/A:1011160810423
Brunetti MT, Peruccacci S, Rossi M et al (2010) Rainfall thresholds for the possible occurrence of landslides in Italy. Nat Hazards Earth Syst Sci 10:447–458. doi:10.5194/nhess-10-447-2010
Byvatov E, Fechner U, Sadowski J, Schneider G (2003) Comparison of support vector machine and artificial neural network systems for drug/nondrug classification. J Chem Inf Comput Sci 43:1882–1889. doi:10.1021/ci0341161
Caine N (1980) The rainfall intensity: duration control of shallow landslides and debris flows. Geografiska Annaler Series A. Phys Geogr 62:23–27. doi:10.2307/520449
Canuti P, Focardi P, Garzonio C (1985) Correlation between rainfall and landslides. Bull Eng Geol Environ 32:49–54. doi:10.1007/BF02594765
Cappa F, Guglielmi Y, Soukatchoff VM et al (2004) Hydromechanical modeling of a large moving rock slope inferred from slope levelling coupled to spring long-term hydrochemical monitoring: example of the La Clapière landslide (Southern Alps, France). J Hydrol 291:67–90. doi:10.1016/j.jhydrol.2003.12.013
Cappa F, Guglielmi Y, Viseur S, Garambois S (2014) Deep fluids can facilitate rupture of slow-moving giant landslides as a result of stress transfer and frictional weakening. Geophys Res Lett 41:61–66. doi:10.1002/2013GL058566
Černý V (1985) Thermodynamical approach to the traveling salesman problem: an efficient simulation algorithm. J Optim Theory Appl 45:41–51. doi:10.1007/BF00940812
Chang C-C, Lin C-J (2011) LIBSVM: a library for support vector machines. ACM Trans Intell Syst Technol 2:1–27. doi:10.1145/1961189.1961199
Chanut M-A, Vallet A, Dubois L, Duranthon J-P (2013) Mouvement de versant de Séchilienne: relations entre déplacements de surface et précipitations—analyse statistique. In: Journées Aléa Gravitaire 2013. Grenoble, France
Corominas J, Moya J, Ledesma A et al (2005) Prediction of ground displacements and velocities from groundwater level changes at the Vallcebre landslide (Eastern Pyrenees, Spain). Landslides 2:83–96. doi:10.1007/s10346-005-0049-1
Cortes C, Vapnik V (1995) Support-vector networks. Mach Learn 20:273–297. doi:10.1007/BF00994018
Cowpertwait PSP, Metcalfe A (2009) Introductory time series with R, Édition: 2009. Springer-Verlag, New York Inc., Dordrecht; New York
Cristianini N (2000) An introduction to support vector machines and other kernel-based learning methods. Cambridge University Press, Cambridge
Crozier MJ (1986) Landslides: causes, consequences et environment. Croom Helm, London, Dover
Durville J-L, Kasperski J, Duranthon J-P (2009) The Séchilienne landslide: monitoring and kinematics. In: First Italian Workshop on Landslides. Napoli, Italia, pp. 174–180
Excoffier JL, Guiochon G (1982) Automatic peak detection in chromatography. Chromatographia 15:543–545. doi:10.1007/BF02280372
Frattini P, Crosta G, Sosio R (2009) Approaches for defining thresholds and return periods for rainfall-triggered shallow landslides. Hydrol Process 23:1444–1460. doi:10.1002/hyp.7269
Fung GM, Mangasarian OL (2004) A feature selection newton method for support vector machine classification. Comput Optim Appl 28:185–202. doi:10.1023/B:COAP.0000026884.66338.df
Guglielmi Y, Vengeon JM, Bertrand C et al (2002) Hydrogeochemistry: an investigation tool to evaluate infiltration into large moving rock masses (case study of La Clapière and Séchilienne alpine landslides). Bull Eng Geol Environ 61:311–324
Guzzetti F, Peruccacci S, Rossi M, Stark CP (2007) Rainfall thresholds for the initiation of landslides in central and southern Europe. Meteorol Atmos Phys 98:239–267. doi:10.1007/s00703-007-0262-7
Guzzetti F, Peruccacci S, Rossi M, Stark CP (2008) The rainfall intensity–duration control of shallow landslides and debris flows: an update. Landslides 5:3–17. doi:10.1007/s10346-007-0112-1
Hastie T (2009) The elements of statistical learning: data mining, inference, and prediction, 2nd edn. Springer, New York
Hsu C-W, Chang C-C, Lin C-J (2003) A practical guide to support vector classification. Department of Computer Science, National Taiwan University, Taipei
Huang J, Lu J, Ling LCX (2003) Comparing Naive Bayes, decision trees, and SVM with AUC and accuracy. In: Proceedings of the third IEEE international conference on data mining. IEEE Computer Society, pp. 553–556
Ivanciuc O (2007) Applications of support vector machines in chemistry. Rev Comput Chem 23:291–400
Iverson RM (2000) Landslide triggering by rain infiltration. W Resour Res 36:1897–1910. doi:10.1029/2000WR900090

Jacobson ML (2001) Auto-threshold peak detection in physiological signals. In: Proceedings of the 23rd Annual International Conference of the IEEE Engineering in Medicine and Biology Society, pp. 2194–2195

Kirkpatrick S, Gelatt CD, Vecchi MP (1983) Optimization by simulated annealing. Science 220:671–680. doi:10.1126/science.220.4598.671

Knight K, Fu W (2000) Asymptotics for Lasso-type estimators. Ann Statist 28:1356–1378. doi:10.1214/aos/1015957397

Le Roux O, Jongmans D, Kasperski J et al (2011) Deep geophysical investigation of the large Séchilienne landslide (Western Alps, France) and calibration with geological data. Eng Geol 120:18–31. doi:10.1016/j.enggeo.2011.03.004

Lebrouc V, Schwartz S, Baillet L et al (2013) Modeling permafrost extension in a rock slope since the last glacial maximum: application to the large Séchilienne landslide (French Alps). Geomorphology 198:189–200. doi:10.1016/j.geomorph.2013.06.001

Li C, Zheng C, Tai C (1995) Detection of ECG characteristic points using wavelet transforms. IEEE Trans Biomed Eng 42:21–28. doi:10.1109/10.362922

Lin H-T, Lin C-J, Weng RC (2007) A note on Platt's probabilistic outputs for support vector machines. Mach Learn 68:267–276. doi:10.1007/s10994-007-5018-6

Madsen H (2007) Time series analysis, 1st edn. Chapman and Hall/CRC, Boca Raton

Martelloni G, Segoni S, Fanti R, Catani F (2012) Rainfall thresholds for the forecasting of landslide occurrence at regional scale. Landslides 9:485–495. doi:10.1007/s10346-011-0308-2

Meric O, Garambois S, Jongmans D et al (2005) Application of geophysical methods for the investigation of the large gravitational mass movement of Séchilienne, France. Can Geotech J 42:1105–1115. doi:10.1139/t05-034

Nafarzadegan AR, Talebi A, Malekinezhad H, Emami N (2012) Antecedent rainfall thresholds for the triggering of deep-seated landslides (case study: Chaharmahal and Bakhtiari Province, Iran). ECO-PERSIA 1:23–39

O'Haver T (1997) A Pragmatic introduction to signal processing. https://terpconnect.umd.edu/~toh/spectrum/TOC.html

Palshikar G (2009) Simple algorithms for peak detection in time-series. In: Proceedings of the 1st International Conference Advanced Data Analysis, Business Analytics and Intelligence

Peruccacci S, Brunetti MT, Luciani S et al (2012) Lithological and seasonal control on rainfall thresholds for the possible initiation of landslides in central Italy. Geomorphology 139–140:79–90. doi:10.1016/j.geomorph.2011.10.005

Platt JC (1999) Probabilistic outputs for support vector machines and comparisons to regularized likelihood methods. In: Advances in large margin classifiers. MIT press, Cambridge, pp. 61–74

Refaeilzadeh P, Tang L, Liu H (2009) Cross-validation. Encycl Database Syst 3:532–538

Rochet L, Giraud A, Antoine P, Évrard H (1994) La déformation du versant sud du Mont-Sec dans le secteur des ruines de Séchilienne (Isère). Bull Int As Eng Geol 50:75–87. doi:10.1007/BF02594959

Rutqvist J, Stephansson O (2003) The role of hydromechanical coupling in fractured rock engineering. Hydrogeol J 11:7–40. doi:10.1007/s10040-002-0241-5

Schölkopf B, Williamson RC, Smola AJ, et al (1999) Support vector method for novelty detection. In: NIPS, pp. 582–588

Segoni S, Rossi G, Rosi A, Catani F (2014) Landslides triggered by rainfall: a semi-automated procedure to define consistent intensity–duration thresholds. Comput Geosci 63:123–131. doi:10.1016/j.cageo.2013.10.009

Stirzaker R, Biggs H, Roux D, Cilliers P (2010) Requisite simplicities to help negotiate complex problems. Ambio 39:600–607. doi:10.1007/s13280-010-0075-7

Tax DMJ, Duin RPW (2004) Support vector data description. Mach Learn 54:45–66. doi:10.1023/B:MACH.0000008084.60811.49

Terlien MTJ (1998) The determination of statistical and deterministic hydrological landslide-triggering thresholds. Environ Geol 35:124–130. doi:10.1007/s002540050299

Vallet A, Bertrand C, Fabbri O, Mudry J (2015a) An efficient workflow to accurately compute groundwater recharge for the study of rainfall-triggered deep-seated landslides, application to the Séchilienne unstable slope (western Alps). Hydrol Earth Syst Sci 19:427–449. doi:10.5194/hess-19-427-2015

Vallet A, Bertrand C, Mudry J et al (2015b) Contribution of time-related environmental tracing combined with tracer tests for characterization of a groundwater conceptual model: a case study at the Séchilienne landslide, western Alps (France). Hydrogeol J 23:1761–1779. doi:10.1007/s10040-015-1298-2

Vallet A, Charlier JB, Fabbri O, et al (2015c) Functioning and precipitation-displacement modelling of rainfall-induced deep-seated landslides subject to creep deformation. Landslides, 1–18. doi: 10.1007/s10346-015-0592-3

Vallet A, Varron D, Bertrand C, Mudry J (2015d) Hydrogeological threshold using support vector machines and effective rainfall applied to a deep seated unstable slope (Séchilienne, French Alps). In: Lollino G, Giordan D, Crosta GB et al (eds) Engineering geology for society and territory, vol. 2. Springer International Publishing, New York, pp 2143–2146

Van Asch TWJ, Buma J, van Beek LP (1999) A view on some hydrological triggering systems in landslides. Geomorphology 30:25–32. doi:10.1016/S0169-555X(99)00042-2

Vengeon JM (1998) Déformation et rupture des versants en terrain métamorphique anisotrope: Apport de l'étude des Ruines de Séchilienne. PhD thesis, Université Joseph Fourier I

Vita PD, Reichenbach P, Bathurst JC et al (1998) Rainfall-triggered landslides: a reference list. Environ Geol 35:219–233. doi:10.1007/s002540050308

Wieczorek GF, Guzzetti F (1999) A review of rainfall thresholds for triggering landslides. In: Proceedings of the EGS Plinius Conference, Maratea, Italy, pp. 407–414

Wilson RC, Wieczorek GF (1995) Rainfall thresholds for the initiation of debris flows at La Honda, California. Environ Eng Geosci 1:11–27

Zhang WJ, Chen YM, Zhan LT (2006) Loading/unloading response ratio theory applied in predicting deep-seated landslides triggering. Eng Geol 82:234–240. doi:10.1016/j.enggeo.2005.11.005